On the dissipative effects in the electron transport through conducting polymer nanofibers

Natalya A. Zimbovskaya

Department of Physics and Electronics, University of Puerto Rico at Humacao,
Humacao, PR 00791, and Department of Physics and Astronomy,
University of Pennsylvania, PA 19104-6323, USA
(Dated: February 6, 2008)

Here, we study the effects of stochastic nuclear motions on the electron transport in doped polymer fibers assuming the conducting state of the material. We treat conducting polymers as granular metals and apply the quantum theory of conduction in mesoscopic systems to describe the electron transport between metalliclike granules. To analyze the effects of nuclear motions we mimic them by a phonon bath, and we include electron-phonon interactions in consideration. Our results show that the phonon bath plays a crucial part in the intergrain electron transport at moderately low and room temperatures, suppressing the original intermediate state for the resonance electron tunneling, and producing new states which support the electron transport. Also, the temperature dependence of magnitudes of the peaks in the electron transmission corresponding to these new states is analyzed.

PACS numbers: 72.15.Gd,71.18.+y

I. INTRODUCTION

Currently, electron transport in conducting polymer nanofibers is a subject of intense interest because such nanofibers are expected to be used in building up nanoelectronic devices. Doped polyacetylen or polyaniline-polyethylene oxide fibers as well as polypyrrole nanotubes could behave as conductors, and their conductivity significantly increases upon doping. Charge transport mechanisms in the conducting polymers were intensively studied starting from the very discovery of these materials [1, 2].

It is known that chemically doped conducting polymers are very inhomogeneous. In some regions polymer chains are disorderly arranged forming an amorphous poorly conducting substance. In other places the chains are ordered and densely packed [3, 4]. The corresponding regions behave as metalliclike grains embedded in the disordered environment. The key point in studies of the electron transport in conducting polymers is to elucidate the nature and physical mechanisms of the intergrain transport. Prigodin and Epstein suggest that the intergrain transport mostly occurs due to the electron tunneling between the grains through intermediate resonance states on the polymer chains connecting them. This approach was employed to build up the theory of electron transport in polyaniline based nanofibers [5] providing a good agreement with the previous transport experiments [6]. Assuming the electron tunneling through the intermediate state to be the predominant mechanism for the intergrain transport, we see a similarity in electron transport mechanisms in conducting polymers and those in molecules connecting metal leads. In the case of polymers metalliclike domains take on part of the leads, and the molecular bridge in between is reduced to a single intermediate site.

An important issue that arises in the analysis of the intergrain electron transport is the influence of nuclear motions in the medium between the grains. The similar issue was analyzed while developing the theory of conduction through macromolecules. It was shown that the environment acts as a source of incoherence for the tunneling electron [7, 8, 9, 10]. Also, it can give rise to some extra electron states [11, 12]. In the previous works [5, 13, 14] the effects of stochastic nuclear motions were analyzed by introducing the coupling of the intermidiate state between the grains to a phonon bath including a large amount of harmonic oscillations. It was shown that the direct coupling of the bridge to the dissipative reservoir (phonon bath) brings an inelastic component to the intergrain transport. This erodes the peak in the electron transmission corresponding to the electron tunneling through the bridge. Nevertheless, estimations made in the recent work [15] give grounds to believe that the peak could be still rather well pronounced under typical conditions of experiments on the electrical characterization of conducting polymer nanofibers.

However, the studies of dissipative effects in the intergrain electron transport in conducting polymers may not be restricted with the plain assumption of the direct coupling of the bridge site to the phonon bath. Other scenarios can occur. In particular, analyzing the electron transport in polymers, as well as in molecules, one must keep in mind that besides the bridge sites there always exist other nearby sites. In some cases the presence of such sites may strongly influence the effects of stochastic nuclear motions on the characteristics of electron transport. This may happen when the nearby sites somehow "screen" the bridge sites from direct interactions with the phonon bath. Here, we elucidate some effects which could appear in the electron transport in conducting polymer fibers in the case of such indirect coupling of the bridge

state to the phonon bath.

II. MODEL AND RESULTS

We mimic the effects of the environment by assuming that the side chain is attached to the bridge, and this chain is affected by the phonon bath. This model resembles those used to analyze electron transport through macromolecules [8, 10, 17]. The side chain is introduced to the model to screen the resonance state making it more stable against the effect of the phonon bath. As in the previous papers [10, 17] we assume that electrons cannot hop along the side chain, so it may be reduced to a single site attached to the resonance site (the bridge).

Within the adopted model the Hamiltonian takes the form:

$$H = H_{el} + H_{ph} + H_{e-ph} + H_L + H_R \quad (1)$$

where the Hamiltonian H_{el} describes the bridge with the attached side site:

$$H_{el} = \epsilon b^+ b + \tilde{\epsilon} c^+ c - w(b^+ c + h.c.), \quad (2)$$

$H_{L,R}$ are self-energy terms describing the coupling of the left (L) and right (R) grain to the bridge, and ϵ and $\tilde{\epsilon}$ are the on-site energies of the bridge site and the attached side site, respectively. The factor w is the hopping integral between the bridge an the attached site.

The remaining terms in the expression (1) describe the phonon bath and the electron-phonon interaction, namely:

$$H_{ph} + H_{e-ph} = \sum_\alpha \Omega_\alpha B_\alpha^+ B_\alpha + \sum_\alpha \lambda_\alpha c^+ c(B_\alpha + B_\alpha^+) \quad (3)$$

where Ω_α are the frequencies of phonons belonging to the bath and λ_α denote the electron-phonon coupling strengths. Performing the unitary transformation $\tilde{H} = e^S H e^{-S}$ with the generator S [16]:

$$S = \sum_\alpha \frac{\lambda_\alpha}{\Omega_\alpha} c^+ c(B_\alpha - B_\alpha^+), \quad (4)$$

the coupling to the bath is eliminated, and we obtain:

$$\tilde{H} = H_{eff} + H_{ph} \quad (5)$$

The effective Hamiltonian for the bridge within the adopted model takes on the form:

$$H_{eff} = \tilde{H}_{el} + H_L + H_R. \quad (6)$$

Here, the Hamiltonian $\tilde{H}_{el}$ may be presented as follows:

$$\tilde{H}_{el} = H_b + H_c + H_{b-c} \quad (7)$$

where again $H_b = \epsilon b^+ b$ corresponds to the bridge site, H_c is the Hamiltonian of the side chain, and H_{b-c} describes the interaction between them. The terms H_c and

H_{b-c} are modified due to the coupling of the side chain to the bath. Keeping only one site in the side chain we have:

$$H_c = (\tilde{\epsilon} - \delta)c^+ c, \quad (8)$$

$$H_{b-c} = -w\chi(b^+ c + h.c.). \quad (9)$$

The quantities δ and χ are given by [10]:

$$\delta = \sum_\alpha \frac{\lambda_\alpha^2}{\Omega_\alpha}, \qquad \chi = \exp\left[\sum_\alpha \frac{\lambda_\alpha}{\Omega_\alpha}(B_\alpha - B_\alpha^+)\right]. \quad (10)$$

The lowest order in the Fourier transform for the Green's function associated with the Hamiltonian (6) reads:

$$G^{-1}(E) = E - \epsilon - \Sigma_L(E) - \Sigma_R(E) - w^2 P(E). \quad (11)$$

The first four terms in this expression represent the inversed Green's function for the resonance site coupled to the two grains where $\Sigma_{L,R}(E)$ are complex self-energy terms. The last term represents the effect of the environment and has the form [10]:

$$P(E) = -i \int_0^\infty dt \exp[it(E - \tilde{\epsilon} + \delta + i0^+)]$$
$$\times \left\{(1 - f) \exp[-F(t)] + f \exp[-F(-t)]\right\} \quad (12)$$

with $\exp[-F(t)]$ being a dynamic bath correlation function, and f taking on values 1 and 0 when the attached site is occupied and empty, respectively.

Characterizing the phonon bath with a continuous spectral density $J(\omega)$ given by [18]:

$$J(\omega) = J_0 \left(\frac{\omega}{\omega_c}\right) \exp\left[-\frac{\omega}{\omega_c}\right], \quad (13)$$

one may write out the following expressions for the functions $F(t)$ and δ:

$$F(t) = \int_0^\infty \frac{d\omega}{\omega^2} J(\omega) \left[1 - e^{-i\omega t} + \frac{2[1 - \cos(\omega t)]}{\exp(\omega/\theta) - 1}\right], \quad (14)$$

$$\delta = \int_0^\infty \frac{d\omega}{\omega} J(\omega) = J_0 \quad (15)$$

where θ is the temperature expressed in the units of energy.

Within the short time scale $(\omega_c t \ll 1)$ the function $F(t)$ could be presented in the form:

$$F(t) = \frac{J_0}{\omega_c} \left\{\frac{1}{2} \ln[1 + (\omega_c t)^2] + i \arctan(\omega_c t) + K(t)\right\} \quad (16)$$

where

$$K(t) = \theta^2 t^2 \zeta\left(2; \frac{\theta}{\omega_c} + 1\right) \equiv \theta^2 t^2 \sum_{n=1}^\infty \frac{1}{(n + \theta/\omega_c)^2}. \quad (17)$$

Here, $\zeta\left(2;\theta/\omega_c + 1\right)$ is the Riemann ζ function [19]. The asymptotic expression for $K(t)$ depends on the relation between two parameters, namely, the temperature θ and the cut-off frequency ω_c characterizing the thermal relaxation rate of the phonon bath. Assuming $\theta \gg \omega_c$ and estimating the sum of the series in Eq. (12) and we get:

$$K(t) \approx \frac{\theta}{\omega_c}(\omega_c t)^2. \qquad (18)$$

In the opposite limit $\omega_c \gg \theta$ we obtain:

$$K(t) \approx \frac{\pi^2}{6}(\theta t)^2 \qquad (19)$$

Also, we may roughly estimate $K(t)$ within the intermediate range. Taking $\theta \approx \omega_c$ we arrive at the approximation $K(t) \approx a^2(\theta t)^2$ where a^2 is a dimensionless constant of the order of unity. Correspondingly, within the short time scale we can omit the first term in the expression (16), and we get:

$$F(t) \approx \frac{J_0}{\omega_c}\left\{i\omega_c t + K(t)\right\} \qquad (20)$$

where $K(t)$ is given by either Eq. (18) or Eq. (19) depending on the relation between ω_c and θ.

Within the long time scale $\omega_c t \gg 1$, and provided that temperatures are not very low ($\theta \gg \omega_c$), we may present the function $K(t)$ as:

$$K(t) = 2\theta t \int_0^\infty \frac{dz}{z^2}(1 - \cos z)e^{-z/\omega_c t} \approx \pi\theta t. \qquad (21)$$

Now, the term $K(t)$ is the greatest addend in the expression for $F(t)$, so the latter could be approximated as: $F(t) \approx \pi\theta t J_0/\omega_c$. The same approximation holds within the low temperature limit when $\omega_c \gg \theta \gg t^{-1}$.

Using the asymptotic expression (20), we may calculate the contribution to $P(E)$ coming from the short time scale ($\omega_c t \ll 1$). It has the form:

$$P_1(E) = -\frac{i}{2}\sqrt{\frac{\pi}{J_0\theta}}\exp\left[-\frac{(E-\tilde\epsilon)^2}{4J_0\theta}\right]\left\{1 + \Phi\left[\frac{i(E-\tilde\epsilon)}{2\sqrt{J_0\theta}}\right]\right\} \qquad (22)$$

where $\Phi(z)$ is the probability integral. When both ω_c and θ have the same order of magnitude the expression for $P(E)$ still holds the form (22). At $\theta \ll \omega_c$, the temperature θ in the expression (22) is to be replaced by ω_c. We remark that under the assumption $\theta \gg \omega_c$ the function $P_1(E)$ does not depend on the cut-off frequency ω_c, whereas at $\omega_c \gg \theta$ it does not depend on temperature. The long time ($\omega_c t \gg 1$) contribution to $P(E)$ could be similarly estimated as follows:

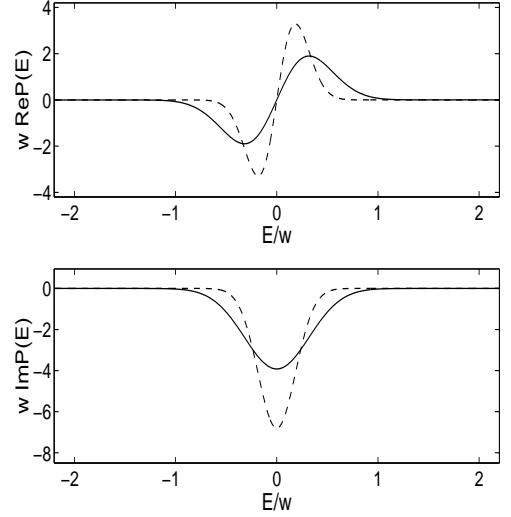$$P_2(E) = \frac{1}{E - \tilde\epsilon + J_0 + i\pi J_0\theta/\omega_c}. \qquad (23)$$

FIG. 1: Energy dependence of the real (top panel) and imaginary (bottom panel) parts of $P(E)$. The curves are plotted assuming $J_0 = 20 meV$, $w = 100 meV$, $\tilde\epsilon = 0$, $T = 100K$ (dash lines), and $T = 300K$ (solid lines) at $\theta \gg \omega_c$.

Comparing these expressions (22) and (23) we see that the ratio of the peak values of $P_2(E)$ and $P_1(E)$ is of the order of $(\omega_c^2/J_0\theta)^{1/2}$. Therefore the term $P_1(E)$ predominates over $P_2(E)$ when the temperatures are moderately high ($\omega_c < \theta$) and the electron-phonon interaction is not too weak $J_0/\omega_c \sim 1$. Usually, experiments on the electrical characterization of conducting polymer nanofibers are carried out at $T \sim 100 \div 300K$, so in further analysis we assume that $(\omega_c^2/J_0\theta)^{1/2} \ll 1$, and we omit the term $P_2(E)$ from the following consideration using the approximation $P(E) \approx P_1(E)$. As shown in the Fig. 1, the imaginary part of $P(E)$ exhibits a dip around $E = \tilde\epsilon$ and the width of the latter is determined by the product of the temperature θ (or ω_c) and the constant J_0 characterizing the strength of the electron-phonon interaction. When either factor increases, the dip becomes broader and its magnitude reduces.

The presence of $P(E)$ gives rise to very significant changes in the behavior of the Green's function given by the Eq. (11). Using the flat band approximation for the self-energy corrections $\Sigma_{L,R}$, namely: $\Sigma_{L,R} = -i\Delta_{L,R}$ where $\Delta_{L,R}$ are constants of the dimensions of energy, and neglecting for a moment all imaginary terms in the Eq. (11), we find that two extra poles of the Green's function emerge due to the environment. When the phonon bath is detached ($J_0 = 0$) the separation between the poles is determined with the hopping integral w. Due to the electron coupling to the phonons the positions of the poles become shifted. Assuming $\epsilon = \tilde\epsilon = 0$ and $\theta \gg \omega_c$ we get:

$$E = \pm 2\sqrt{J_0\theta|\ln(2J_0\theta/w^2)|}. \qquad (24)$$

The poles correspond to extra electron states which occur due to electrons coupling to the environment. These new states are revealed in the structure of the electron transmission $T(E)$ which reads [20]:

$$T(E) = 4\Delta_L \Delta_R |G(E)|^2. \tag{25}$$

The structure of $T(E)$ is shown in the Fig. 2. Two peaks in the transmission are associated with the environment induced electronic states. Their positions and heights depend on the temperature and on the coupling strengths J_0, and w. The important feature in the electron transmission is the absence of the peak associated with the resonance state between the grains (the bridge site) itself. This happens due to the strong suppression of the latter by the effects of the environment. Technically, this peak is damped for it is located at $E = 0$ where the imaginary part of $P(E)$ reaches its maximum in magnitude. To provide the damping of the original resonance the contribution from the environment (including the side chain attached to the bridge) to the Green's function (11) must exceed the terms $\Sigma_{L,R}$ describing the effect of the grains. This occurs when the inequality

$$\Delta < w^2/\sqrt{J_0 \theta} \tag{26}$$

is satisfied. When the coupling of the bridge to the attached side site is weak, the influence of the environment slackens and the original peak associated with the bridge at $E = \tilde{\epsilon}$ may emerge. At the same time the features originating from the environment induced status become small compared to this peak.

So, the effects of the environment may lead to the damping of the original resonance state for the electron tunneling between the metallic islands in the polymer fiber. Instead, two environment induced states appear to serve as intermediate states for the electron transport. Similar effects were recently investigated in the electron transport through DNA macromolecules [10], and it was shown that low biased current-voltage characteristics may be noticeably changed due to the occurence of the phonon bath induced electron states. Due to some particular features of conducting polymers, these effects may be revealed in polymer nanofiber current-voltage curves at significantly higher bias voltage, as discussed below.

Realistic polymer nanofibers have diameters within the range $20 \div 100$ nm, and lengths of the order of a few microns. This is much greater than the typical size of both metalliclike grains and intergrain separations which take on values $\sim 5 \div 10$ nm [21]. Therefore, we may treat a nanofiber as a set of parallel working channels, any single channel being a sequence of grains connected with the resonance polymeric chains. The net current in the fiber is the sum of currents flowing in these channels, and the voltage V applied across the whole fiber is distributed among sequential pairs of grains along a single channel.
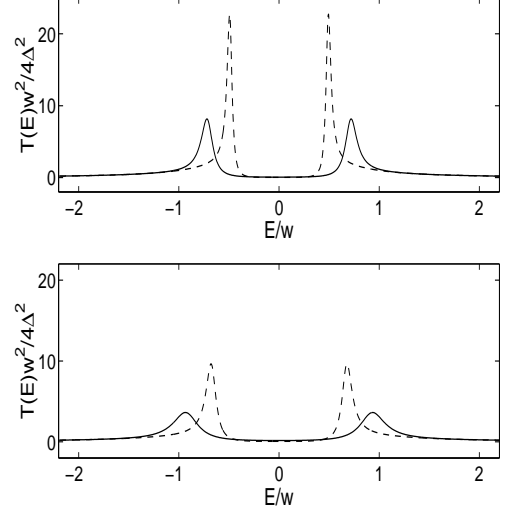

FIG. 2: The renormalized electron transmission function vs energy. The curves are plotted for $\epsilon = \tilde{\epsilon} = 0$, $w = 100 meV$, $T = 100K$ (dash lines) and $T = 300K$ (solid lines). The constant J_0 equals $20 meV$ (top panel) and $50 meV$ (bottom panel).

So, the voltage ΔV applied across two adjacent grains could be estimated as $\Delta V \sim V L/L_0$ where L is the average separation between the grains, and L_0 is the fiber length. The ratio $\Delta V/V$ may take on values of the order of $10^{-1} \div 10^{-2}$. Experiments on the electrical characterization of the polymer fibers are usually carried out at moderately high temperatures ($T \div 300K$), so it seems likely that $\theta > \omega_c$. Assuming that $w \sim 100 meV$, and $J_0 \sim 20 \div 50 meV$ we estimate the separation between the environment induced peaks in the electron transmission as $120 \div 170 meV$ (see Fig. 2). This estimate is close to $e\Delta V$ when V takes on values up to $2 \div 3$ volts. So, the environment induced peaks in the electron transmission determine the shape of the current-voltage curves even at reasonably high values of the bias voltage applied across the fiber.

In calculations of the current we employ the formula [20]:

$$I = \frac{2en}{h} \int_{-\infty}^{\infty} dE T(E)[f_1(E) - f_2(E)]. \tag{27}$$

Here, n is the number of the working channels in the fiber, $f_{1,2}(E)$ are Fermi functions taken with the different contact chemical potentials $\mu_{1,2}$ for the grains. The chemical potentials differ due to the applied bias voltage ΔV:

$$\mu_1 = E_F + (1 - \eta)e\Delta V; \qquad \mu_2 = E_F - \eta e\Delta V. \tag{28}$$

The parameter η characterizes how the voltage ΔV is divided between the grains; E_F is the equilibrium Fermi
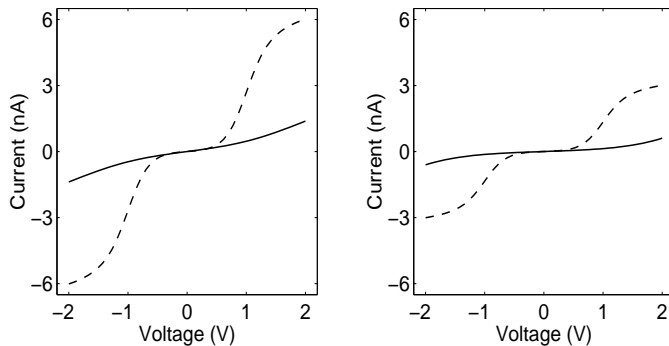
FIG. 3: The current-voltage characteristics (nA–V) plotted for $n = 10$, $\Delta_L = \Delta_R = 0.5 meV$, $\eta = 1/2$, $w = 100 meV$, $J_0 = 20 meV$ (left panel), and $J_0 = 50 meV$ (right panel) at $T = 100K$ (dash lines) and $T = 300K$ (solid lines).

FIG. 4: Arrhenius plot of the peak value of the electron transmission function for $J_0 = 20 meV$, $w = 100 meV$, $\Delta_L = \Delta_R = 0.5 meV$; $\theta_0 = 8.6 meV$ ($T = 100K$). Solid line is plotted assuming the indirect coupling of the bridge to the phonon bath (Eqs. (11), (25)). Dashed line is plotted assuming that the bridge is directly coupled to the phonons (Eq. (29)).

energy of the system including the pair of grains and the resonance site in between, and $T(E)$ is the electron transmission function given by Eq. (25).

The resulting current-voltage characteristics are shown in the Fig. 3. The current takes on low values ($\sim 1nA$) because the coupling of the grains to the intermediate state is weak due to comparatively large distances between the grains [2]. Consequently, $\Delta_{L,R}$ take on values much smaller than those typical for electron transport through molecules placed between metal leads. The $I-V$ curves exhibit a nonlinear shape even at room temperature despite the fact that the original state for the resonance tunneling is completely suppressed. This occurs for the intergrain transport is supported by new phonon induced electron states. In this work we did not take a task of providing a quantitative agreement between the theory and experimental results obtained on conducting polymer fibers. However, in general, our calculated $I-V$ curves agree with the reported experiments [7].

It is worthwhile to discuss the temperature dependence of the peak value of the electron transmission which follows from the present results. Using the expression (11) for the Green's function and the expression (22) for $P(E)$ we may conclude that at low temperatures the transmission accepts small values, and exhibits rather weak temperature dependence. At higher temperatures ($T \sim 100K$) the transmission increases fast as the temperature rises and then it reduces as the temperature further increases. The peak in the transmission is associated with the most favorable conditions for the environment induced states to exist when all remaining parameters (such as J_0 and w) are fixed. At high temperatures the peaks associated with the environment induced states are washed out, as usual. This is shown in the Fig. 4. Also, basing on the results of the previous works [5, 15] we may analyze the temperature dependence of the electron transmission function assuming that the bridge between
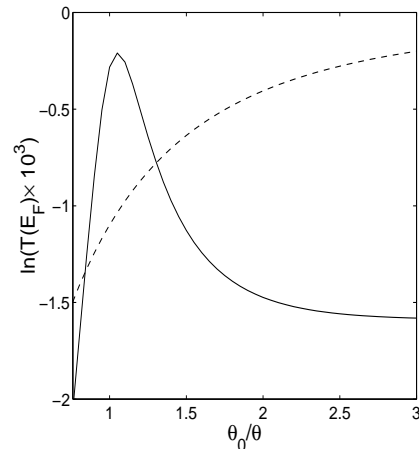
two adjacent grains is directly coupled to the phonon bath. In this case the transmission peak value may be presented in the form [15]:

$$T(E) = 1 - \frac{\rho^4}{2(1 + \sqrt{1 + \rho^2})^2} \qquad (29)$$

where

$$\rho^2 = \frac{16J_0}{\omega_c} \frac{\theta^2}{(\Delta_L + \Delta_R)} \zeta\left(2; \frac{\theta}{\omega_c} + 1\right). \qquad (30)$$

The temperature dependence of the transmission given by the Eq. (29) is also shown in the Fig. 4. Both curves are plotted at the same value of the electron-phonon coupling strength J_0. Comparing them we conclude that at higher temperatures the curves appear to differ. While the temperature rises, we observe a peak in the electron transmission assuming the indirect coupling of the bridge to the phonon bath, and we see the transmission to monotonically decrease when we consider the bridge directly coupled to the bath. Correspondingly, we may expect qualitative diversities to appear in the temperature dependencies of the current, as well. These diversities originate from the difference in the effects of environment on the intergrain electron transport in the cases of direct and indirect coupling of the bridge site to the phonon reservoir. When the bridge is directly coupled to the bath the stochastic motions in the environment only cause the peak in the electron transmission to be eroded, and the higher is the temperature the less distinguishable is the peak. However, when the bridge is screened from the direct coupling with the phonons due to the presence of the nearby sites, the stochastic nuclear motions in the medium between the grains (especially those

in the resonance chain) may take a very different part in the electron transport in conducting polymers at moderately low and room temperatures. Due to their influence the original intermediate state for the resonance tunneling may be completely suppresed but new environments induced states may appear providing the electron transport through the polymer nanofibers.

III. CONCLUSION

Finally, studies of the electron transport in conducting polymers are not completed so far. There are solid grounds to expect significant dissipative effects in the intergrain transport at moderately high temperatures. As shown in the previous studies of the electron transport through molecules, various dissipative effects may occur depending on characteristic features in the interaction of a propagating electron with the environment. Among these features we may single out the character of the electron coupling to the dissipative reservoir (phonon bath) as a very significant factor. It is likely that in realistic conducting polymers both direct and indirect coupling of the intermediate state (the bridge) to the environment may occur. We need more experimental data concerning transport in these materials to determine which kind of coupling would prevail in a particular material under particular experimental conditions. The model adopted in the present work predicts that the temperature dependence of the electron transmission through the environment induced states crucially differs from that which is typical for the electron transport through the original bridge state directly coupled to the dephasing reservoir. So, the present results give means to experimentaly study distinctive features of the dissipative effects in the electron transport through conducting polymer nanofibers.

[1] A. G. MacDiarmid, Rev. Mod. Phys. **73**, 701 (2001).
[2] See e.g. V. N. Prigodin and A. J. Epstein, Synth. Met. **125**, 43 (2002) and references therein.
[3] J. Joo, Z. Oblakowski, G. Du, J. P. Ponget, E. J. Oh, J. M. Wiessinger, Y. Min, A. G. MacDiarmid, and A. J. Epstein, Phys. Rev. B **49**, 2977 (1994).
[4] J. P. Ponget, Z. Oblakowski, Y. Nogami, P. A. Albony, M. Laridjani, E. J. Oh, Y. Min, A. J. MacDiarmid, J. Tsukamoto, T. Ishiguro, and A. J. Epstein, Synth. Met. **65**, 131 (1994).
[5] N. A. Zimbovskaya, A. T. Johnson Jr., and N. J. Pinto, Phys. Rev. B **72**, 024213 (2005).
[6] Yangxin Zhou, M. Freitag, J. Hone, C. Stali, A. T. Johnson Jr., N. J. Pinto, and A. G. MacDiarmid, Appl. Phys. Lett. **83**, 3800 (2003).
[7] A. Nitzan, Ann. Rev. Phys. Chem. **52**, 681 (2001).
[8] X. Q. Li and Y. Yan, Appl. Phys. lett. **81**, 925 (2001).
[9] M. Galperin, A. Ratner, and A. Nitzan, J. Chem. Phys. **121**, 11965 (2004).
[10] R. Gutierrez, S. Mandal, and G. Cuniberti, Phys. Rev. B **71**, 235116 (2005).
[11] R. G. Endres, D. L. Cox, and R. R. P. Singh, Rev. Mod. Phys. **76**, 195 (2004).
[12] F. L. Gervasio, P. Carloni, and M. Partinello, Phys. Rev. Lett. **89**, 108102 (2002).
[13] N. A. Zimbovskaya, J. Chem. Phys. **123**, 114708 (2005).
[14] M. Buttiker, Phys. Rev. B **33**, 3020 (1986).
[15] N. A. Zimbovskaya, cond-mat/0608591.
[16] U. Weiss, Quantum Dissipative Systems, Vol. 10 in *Series in Modern Condesed Matter Physics* (World Scientific, Singapore, 1999).
[17] G. Cuniberti, L. Craco, D. Porath, and C. Dekker, Phys. Rev. B **65**, 241314(R) (2002).
[18] G. D. Mahan, *Many-Particle Physics* (Plenum, New York, 2000).
[19] I. S. Gradshteyn and I. M. Ryzhik, *Tables of Integrals, Series and Products* (Academic, New York, 2000).
[20] S. Datta, *Electronic Transport in Mesoscopic Systems* (Cambridge University Press, Cambridge, England, 1995).
[21] See e.g. R. Pelster, G. Nimtz, and B. Wessling, Phys.Rev. B **49**, 12718 (1994).